THE JOURNAL OF BIOLOGICAL CHEMISTRY VOL. 289, NO. 11, pp. 7825–7834, March 14, 2014

Evidence That the DNA Endonuclease ARTEMIS also Has Intrinsic 5′-Exonuclease Activity*

Received for publication, December 26, 2013, and in revised form, January 27, 2014 Published, JBC Papers in Press, February 5, 2014, DOI 10.1074/jbc.M113.544874

Sicong Li[‡], Howard H. Chang[‡], Doris Niewolik[§], Michael P. Hedrick[¶], Anthony B. Pinkerton[¶], Christian A. Hassig[¶], Klaus Schwarz[§], and Michael R. Lieber[‡1]

From the [‡]Departments of Pathology, Biochemistry and Molecular Biology, Biological Sciences, and Molecular Microbiology and Immunology, University of Southern California Keck School of Medicine, Norris Comprehensive Cancer Center, Los Angeles, California 90089-9176, the [§]Institute for Transfusion Medicine, University Hospital, D-89081 Ulm, Germany, and the [¶]Sanford Burnham Medical Research Institute, La Jolla, California 92037

Background: DNA-PKcs stimulates the endonucleolytic activities of ARTEMIS but not the 5′-exonuclease activity.
Results: Point mutagenesis, small molecule inhibitors, and modulation of divalent cation concentrations all affect both the endonuclease and 5′-exonuclease activities in parallel.
Conclusion: ARTEMIS has intrinsic 5′-exonuclease activity, in addition to its known endonuclease activity.
Significance: ARTEMIS may use both its endo- and its 5′-exonuclease activity in NHEJ.

ARTEMIS is a member of the metallo-β-lactamase protein family. ARTEMIS has endonuclease activity at DNA hairpins and at 5′- and 3′-DNA overhangs of duplex DNA, and this endonucleolytic activity is dependent upon DNA-PKcs. There has been uncertainty about whether ARTEMIS also has 5′-exonuclease activity on single-stranded DNA and 5′-overhangs, because this 5′-exonuclease is not dependent upon DNA-PKcs. Here, we show that the 5′-exonuclease and the endonuclease activities co-purify. Second, we show that a point mutant of ARTEMIS at a putative active site residue (H115A) markedly reduces both the endonuclease activity and the 5′-exonuclease activity. Third, divalent cation effects on the 5′-exonuclease and the endonuclease parallel one another. Fourth, both the endonuclease activity and 5′-exonuclease activity of ARTEMIS can be blocked in parallel by small molecule inhibitors, which do not block unrelated nucleases. We conclude that the 5′-exonuclease is intrinsic to ARTEMIS, making it relevant to the role of ARTEMIS in nonhomologous DNA end joining.

ARTEMIS is a member of the metallo-β-lactamase superfamily of nucleases. The metallo-β-lactamase family is characterized by a conserved metallo-β-lactamase and β-CASP[2] domain and their ability to hydrolyze DNA or RNA. Two other mammalian members of the same family, SNM1A and SNM1B (Apollo), function in DNA interstrand cross-link repair (1) and protection of telomeres (2). ARTEMIS, also known as SNM1C, functions in the nonhomologous end joining (NHEJ) repair pathway. On duplex DNA, ARTEMIS has endonuclease activity on 5′- and 3′-DNA overhangs and at DNA hairpins, and these are all dependent on DNA-PKcs (3). In the context of V(D)J recombination, the ARTEMIS·DNA-PKcs complex is required for the opening of hairpins generated by the RAG complex (3). Patients lacking ARTEMIS suffer from severe combined immunodeficiency (4). NHEJ requires nucleases for resection of broken DNA ends, polymerase to fill in the gaps, and the XLF·XRCC4·DNA ligase IV complex for ligation (5). ARTEMIS is at least one of the nucleases participating in this process and is responsible for a subset of end processing during NHEJ in response to ionizing radiation (6). Patients or cells lacking ARTEMIS are deficient for repair caused by ionizing radiation (4, 7) and for repair of breaks caused by topoisomerase II inhibitors (8).

In a biochemical system consisting of purified proteins of the NHEJ pathway, ARTEMIS, in complex with the serine/threonine kinase DNA-PKcs, removes 5′- and 3′-overhangs in order to join duplex DNA ends (9). ARTEMIS·DNA-PKcs is also able to open hairpins both *in vivo* and *in vitro*. ARTEMIS opens hairpins preferentially two nucleotides past the tip of a perfect hairpin (3). At a 5′-overhang, ARTEMIS·DNA-PKcs preferentially cuts directly at the double-stranded/single-stranded junction (3, 10). At a 3′-overhang, ARTEMIS preferentially cuts 4 nucleotides into the single-stranded overhang from the double/single-stranded DNA junction (11). All of the endonuclease activities of ARTEMIS on duplex DNA ends can be unified by a model invoking binding to the single- to double-stranded junction and occupying 4 nt along the single-stranded portion, followed by nicking preferentially 3′ of those 4 nt (3).

In addition to its endonucleolytic action on the single-strand to double-stranded transitions (overhangs and hairpins of duplex DNA), ARTEMIS alone has a weaker single-stranded DNA endonuclease activity, such as on poly(dT) (12). Similar to the endonuclease activity of ARTEMIS on duplex DNA substrates, the action of ARTEMIS on entirely single-stranded DNA is stimulated by the addition of DNA-PKcs (12), which forms a complex with ARTEMIS that is stable to well over 0.5 M monovalent salt (3). Our model for ARTEMIS endonucleolytic

* This work was supported by a National Institutes of Health Grants R01 CA100504 and R01 CA51105 (to M. R. L.) and the BMBF (German Federal Ministry of Education & Research) Grant 01GM1111F (to K. S.).
[1] To whom correspondence should be addressed. Tel.: 323-865-0568; E-mail: lieber@usc.edu.
[2] The abbreviations used are: β-CASP, β-lactamase, CPSF (cleavage and polyadenylation specificity factor), Artemis, Snm1, Pso2 domain; NHEJ, nonhomologous DNA end joining; DNA-PKcs, DNA-dependent protein kinase, catalytic subunit; ssDNA, single-stranded DNA; Ni-NTA, nickel-nitrilotriacetic acid.

action on single-stranded DNA (ssDNA) proposes binding by ARTEMIS at random locations along the ssDNA, followed by nicking, and these activities of ARTEMIS are increased by DNA-PKcs.

Purified ARTEMIS protein also appears to have 5′-exonuclease activity, which is DNA-PKcs-independent (3). The 5′-exonuclease activity co-fractionates with the known endonucleolytic activities of ARTEMIS (12). Exonucleases are abundant in cells and are common contaminants. As other 5′-exonucleases are purified away, the apparent level of 5′-exonuclease activity falls, but not to zero, and the question arises whether the residual level of 5′-exonuclease activity is intrinsic to ARTEMIS or a contaminating enzyme that co-fractionates with ARTEMIS.

Similar to other members of the metallo-β-lactamase family, it is thought that ARTEMIS requires the binding of divalent cations to two co-catalytic portions of the active site for catalysis (13). Each catalytic site may hold one Mg^{2+}, Mn^{2+}, or Zn^{2+} ion. In the metallo-β-lactamase family, the ligands for the divalent cations are generally conserved and consist of a combination of histidine and aspartic acid residues (14). Our previous studies have demonstrated that upon mutation of these conserved residues, the endonuclease activity of ARTEMIS·DNA-PKcs can be markedly reduced. However, the 5′-exonuclease activity appeared to remain (13). This raised the possibility that the 5′-exonuclease activity and the endonuclease activity of ARTEMIS use two independent catalytic sites. However, an alternative explanation is that previous attempts at testing point mutants were carried out using 293T cells, a system known for high levels of background nucleases, and complete removal of contaminating 5′-exonucleases may not have been successful.

Here, we present a point mutant of ARTEMIS created using a baculovirus expression system, a system that more readily permits purification away from host cell 5′-exonucleases. This mutation markedly reduces both the endonuclease as well as the 5′-exonuclease activities of ARTEMIS. We have also identified small molecules that inhibit both the ARTEMIS endonuclease and 5′-exonuclease activities in parallel. These and other findings shed light on ARTEMIS nuclease activity and expand the range of substrates that ARTEMIS can act upon. We discuss these findings in the context of NHEJ.

EXPERIMENTAL PROCEDURES

Oligonucleotides and DNA Substrates—Oligonucleotides used in this study were synthesized by Operon Biotechnologies, Inc. (Huntsville, AL) and Integrated DNA Technologies, Inc. (San Diego, CA). We purified the oligonucleotides using 12 or 15% denaturing PAGE and determined the concentration spectrophotometrically. DNA substrate 5′ end-labeling was done with [γ-^{32}P]ATP (3000 Ci/mmol) (PerkinElmer Life Sciences) and T4 polynucleotide kinase (New England Biolabs) according to the manufacturer's instructions. Substrates were incubated with [γ-^{32}P]ATP and T4 PNK for 30 min at 37 °C. T4 PNK was subsequently inactivated by incubating samples at 72 °C for 20 min. Unincorporated radioisotope was removed by using G-25 Sephadex (Amersham Biosciences, Inc.) spin column chromatography. For the hairpin substrate, YM164-labeled oligonucleotide was diluted in a buffer containing 10 mM Tris-HCl (pH 8.0), 1 mM EDTA (pH 8.0), and 100 mM NaCl, heated at 100 °C for 5 min, allowed to cool to room temperature for 3 h, and then incubated at 4 °C overnight. The sequences of the oligonucleotides used in this study are as follows: JG 169, 5′-TTT TTT TTT TTT TTT TTT TTT TTT TTT-3′; JG 167, 5′-AAA AAA AAA AAA AAA AAA AAA AAA AAA-3′; YM164, 5′-TTT TTG ATT ACT ACG GTA GTA GCT ACG TAG CTA CTA CCG TAG TAA T-3′; and SL 23, 5′-T*T*T*T*TT TTG CCA GCT GAC GCG CGT CAG CTG GC-3′, where the *asterisk* designates phosphothioate bonds.

Protein Expression and Purification—ARM14 recombinant baculovirus with a C-terminal His_8 tag was cloned into baculodirect vector and transfected into Sf21 according to protocol (Invitrogen). Virus was harvested after 48 h and used to infect Sf9 cells in log phase growth. Wild type ARTEMIS was purified as described previously (12). Harvested ARM14-infected Sf9 cells were resuspended in Ni-NTA binding buffer (50 mM NaH_2PO_4 (pH 7.8), 0.5 M KCl, 2 mM β-mercaptoethanol, 10% glycerol, 0.1% Triton X-100, and 20 mM imidazole (pH 7.8)) supplemented with protease inhibitors. Cells were lysed by sonication and applied to Ni-NTA-agarose resin (Qiagen). Bound ARM14 protein was eluted off using 250 mM imidazole. Eluted protein was directly applied to DEAE-Sepharose resin (GE Healthcare). Unbound soluble fraction was collected and dialyzed against Superose 12 buffer (500 mM KCl, 25 mM Tris-HCl, 1 mM DTT). ARM14 fractions eluted from Superose 12 were frozen down and stored at −80 °C. Expression and purification of DNA-PKcs from HeLa cells has been described previously (15).

Circular Dichroism—All CD studies were conducted on Jasco-810 Spectro Polarimeter. A wavelength of 260 nm was used at the start and 190 nm for the end reading. A data pitch of 0.5 nm was used with continuous reading and 20 accumulations per scan.

Biochemical Nuclease Assay—The *in vitro* DNA nuclease assay was performed in a volume of 10 μl with a buffer composition of 25 mM Tris-HCl (pH 7.5), 10 mM KCl, 10 mM $MgCl_2$, and 1 mM DTT. In the reaction, 50 nM single-stranded DNA or 20 nM hairpin DNA YM164 or SL23 was mixed with 50 nM ARM14 or 50 nM wild-type ARTEMIS. In specified cases, 10 mM $MnCl_2$ replaced 10 mM $MgCl_2$. In specified cases, 50 nM DNA-PKcs was added with 0.5 mM ATP. DNase I and micrococcal nuclease were obtained from New England Biolabs and Sigma, respectively. Reactions were then incubated at 37 °C for 1 h. After incubation, reactions were stopped and analyzed on a 12% denaturing PAGE.

Cells and Transfection—HEK293T cells were transfected by nucleofection using AMAXA nucleofector kit V (Lonza). Equal transfection efficiencies were confirmed by co-transfection of an enhanced green fluorescent protein expression plasmid followed by FACS analysis.

Immunoprecipitation and Immunoblotting—The immunoprecipitation was performed as described (3). Myc-tagged ARTEMIS was immunoprecipitated and detected with anti-Myc antibody (Invitrogen). SV40 large T antigen was used as loading control and was detected with anti-SV40 T-Ag antibody (Santa Cruz Biotechnology, Santa Cruz, CA). Endogenous

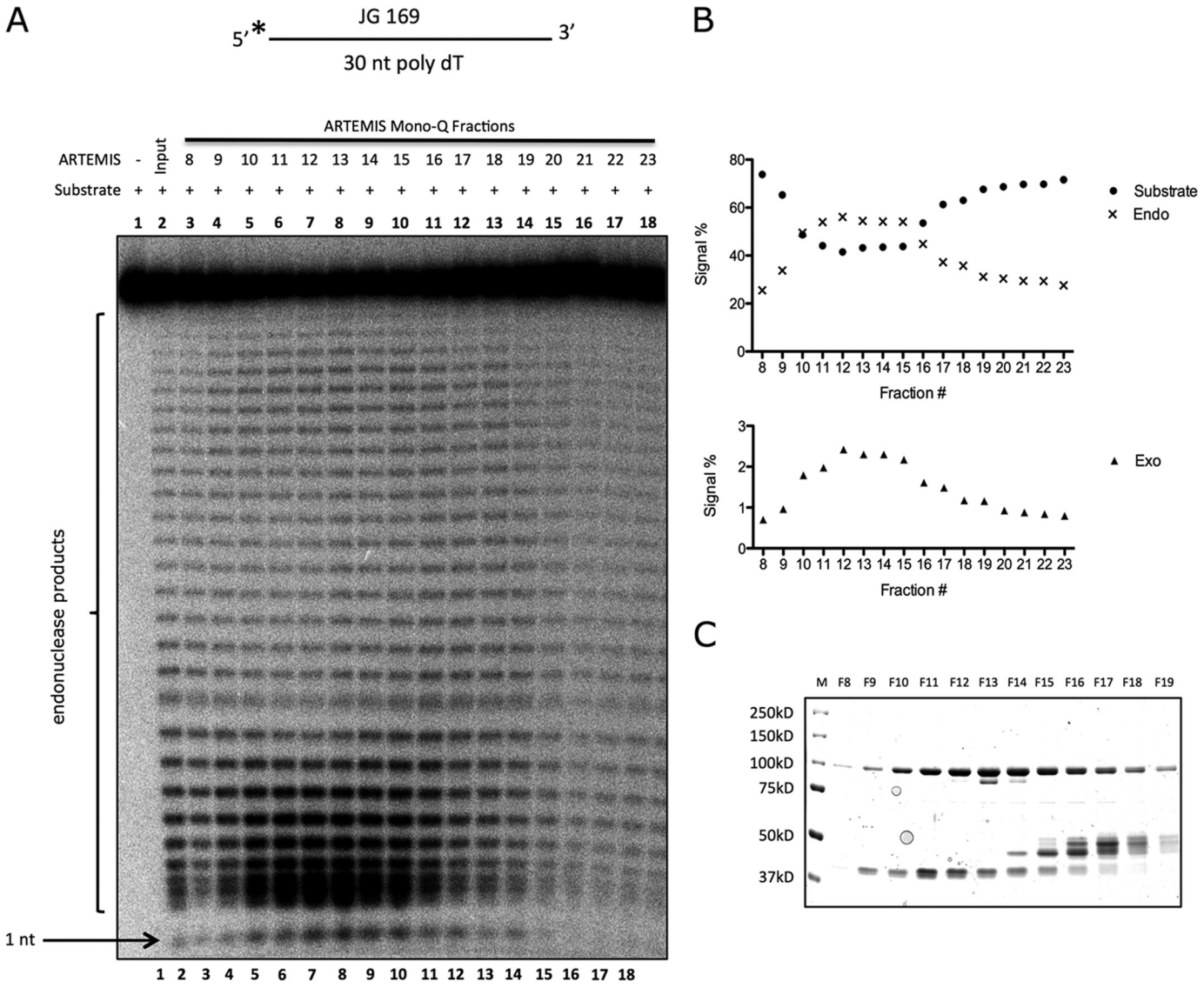

FIGURE 1. **Mono Q-purified ARTEMIS exonuclease activity correlates with its endonuclease activity.** *A*, 20 nM of 5′-radiolabeled (designated by *asterisk*) ssDNA substrate (JG169) was incubated with 1 μl of Mono Q fractions in a 10-μl reaction. The reaction was performed in 25 mM Tris-Cl (pH 8.0), 10 mM $MnCl_2$, 50 μg/ml BSA, and 1 mM DTT for 60 min at 37 °C. *Lane 2* contains pre-Mono Q ARTEMIS, and *lanes 3–18* contain Mono Q fractions 8–23. The 5′-exonuclease activity is seen as the 1-nt product at the *bottom* of the gel. *B*, the signals of remaining substrate (30-nt position), endonucleolytic products (2–29-nt position), and exonucleoytic product (1-nt position) were quantified by boxing the corresponding bands and measuring the summed band intensities using Bio-Rad Quantify One software. The signal % was plotted as a function of fraction number. The *top graph* plots the substrate and endonucleolytic product signals. The *bottom graph* plots the 5′-exonucleolytic product signal. *C*, an SDS-PAGE gel is stained with Coomassie Blue. The gel shows that purified Artemis from the Mono Q column runs at the 100-kDa position. Fractions 10–18 correlate with peak activity as well as ARTEMIS protein abundance.

DNA-PKcs was detected using anti-DNA-PKcs antibody (Abcam).

RESULTS

ARTEMIS Endonuclease and 5′-Exonuclease Activities Co-purify with WT ARTEMIS Protein—ARTEMIS has a well documented set of endonuclease activities, all of which are stimulated by DNA-PKcs (3). The 5′-exonuclease activity of ARTEMIS co-fractionates with the ARTEMIS endonucleolytic activities (Fig. 1). The 5′-exonuclease activity is seen as the 1-nt product at the bottom of Fig. 1*A*. The 5′-exonuclease activity is not stimulated by DNA-PKcs (3), and for this reason, we wondered whether the 5′-exonuclease is intrinsic to ARTEMIS.

Expression and Purification of ARM14 Point Mutant—We created a point mutant of ARTEMIS by mutating the conserved histidine at amino acid 115 to an alanine (Fig. 2*A*). The histidine at amino acid 115 is a putative binding site for divalent cations involved in the catalysis of DNA (13). This was subsequently cloned into a baculodirect vector (Invitrogen) to generate what we call the ARM14 baculovirus and mutant form of ARTEMIS protein. The ARM14 mutant and WT human ARTEMIS-His proteins were both expressed in Sf9 insect cells using a baculovirus expression system. Both the WT and ARM14 mutant proteins were purified using Ni-NTA, an anion exchange step, followed by a Superose 12 gel filtration column. Purified ARM14 mutant elutes as a relatively sharp peak off of the Superose 12 column and runs at 100 kDa on 8% SDS-PAGE (Fig. 2, *B* and *D*). The ARM14 mutant runs at the same position (~100 kDa) as the WT ARTEMIS on 8% SDS-PAGE (Fig. 2*C*).

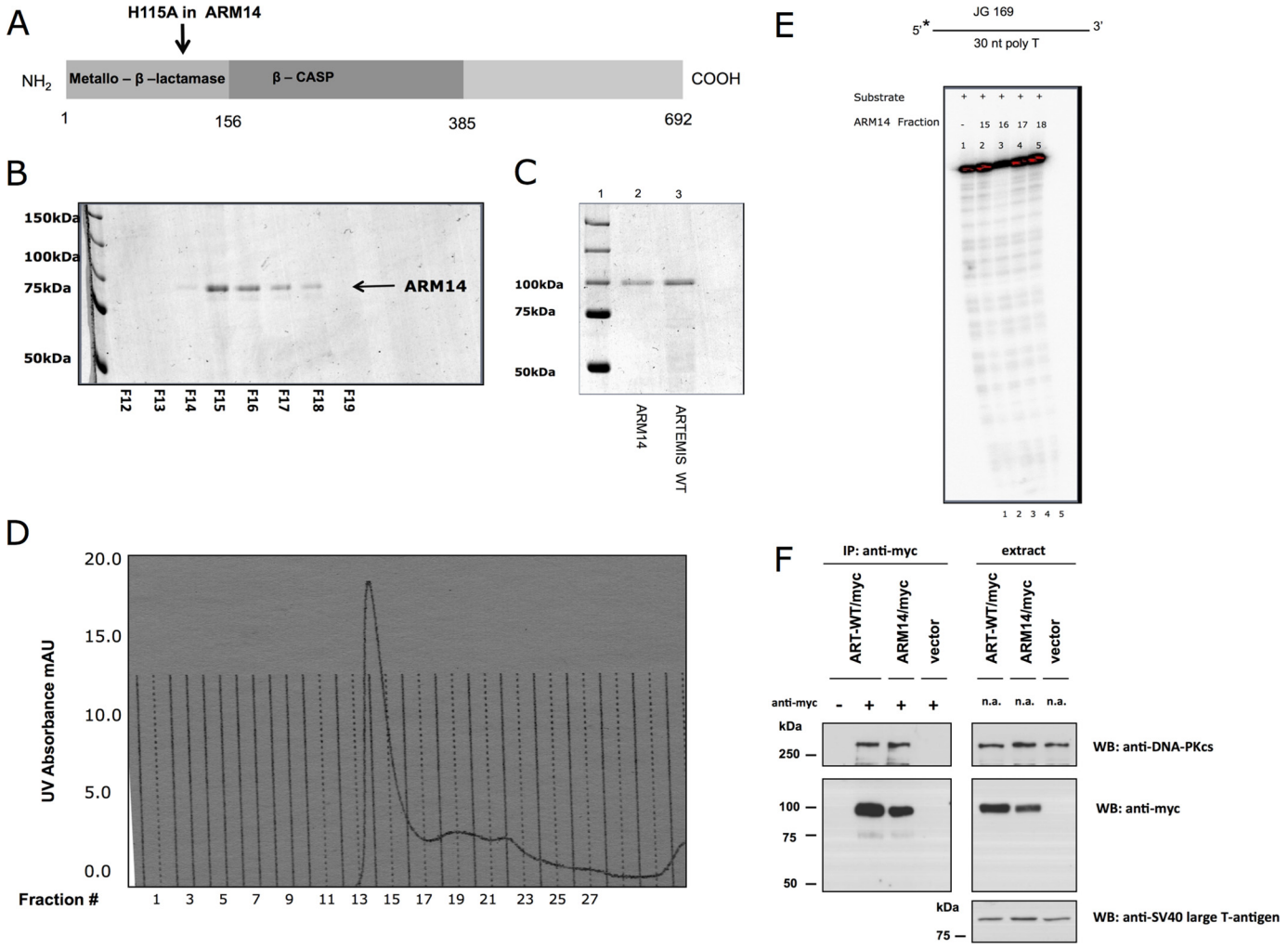

FIGURE 2. **Size exclusion chromatography and characterization of a single amino acid point mutant of ARTEMIS, the ARM14 mutant.** *A*, the ARM14 mutant was constructed by creating a point mutation in the putative active site of ARTEMIS, specifically histidine 115 to alanine, followed by cloning into a baculodirect vector. *B*, an SDS-PAGE gel was stained with Coomassie Blue. The gel shows that the ARM14 mutant protein has a gel mobility of ~100 kDa. *C*, ARM14 and wild type ARTEMIS were both run on an 8% SDS-PAGE gel and stained with Coomassie Blue. Purified ARM14 mutant (*lane 2*) and wild type ARTEMIS (*lane 3*) have gel mobility positions at ~100 kDa, 2 μg of each was loaded onto the SDS-PAGE. The molecular weight marker is in *lane 1*. *D*, the UV profile of ARM14 during Superose 12 size exclusion chromatography is shown. Purified ARM 14 mutants elutes as a ~450-kDa multimer at fraction 15 on the Superose 12 size exclusion column. *E*, fractions across the Superose 12 UV peak were collected and assayed for nuclease activity. In each reaction, 50 nM of ARM14 mutant was incubated with 50 nM of ssDNA poly(dT) substrate (JG169) in a 10-μl reaction. Reactions were incubated for 60 min at 37 °C (see "Experimental Procedures" for standard reaction solution composition here and for subsequent gels, except where specified otherwise), stopped, and run on 12% denaturing PAGE. The ARM14 mutant fractions 15–18 do not show any endonuclease or 5′-exonuclease activity. *F*, ARM14 binds endogenous DNA-PKcs. Empty vector (*EV*), wild type (ART-WT), or mutant ARTEMIS (ARM14) expressing plasmids were transfected into HEK293T cells, and the Myc-tagged ART-WT/ARM14 was immunoprecipitated (*IP*) in the presence (+) or absence (−) of anti-Myc antibody from cell lysates. *n.a.*, not applicable. ART-WT/ARM14, co-precipitated endogenous DNA-PKcs, and the loading control SV40 large T-antigen were detected with the corresponding antibodies by Western blot (*WB*) analysis. The position of protein standards is shown at the *left* in kDa. Transfection efficiencies were between 83 and 86%. *mAU*, milliabsorbance units.

To ensure that the ARM14 mutant was not denatured, we used circular dichroism (CD) on the WT ARTEMIS, on ARM14, and on completely heat-denatured ARTEMIS. The WT ARTEMIS and ARM14 had similar CD profiles (data not shown). Hence, purified ARM14 mutant has a conformation that is indistinguishable from WT ARTEMIS by CD.

Additionally, we performed a pulldown experiment to assess the ability of ARM14 protein to bind to endogenous DNA-PKcs. ARTEMIS or ARM14 expression plasmids were transfected into HEK293T cells. Myc-ARTEMIS and Myc-ARM14 were immunoprecipitated using anti-Myc antibody. We assayed to determine whether DNA-PKcs was also co-immunoprecipitated in both cases. The presence of DNA-PKcs was assayed using anti-DNA-PKcs antibody. We find that the ARM14 point mutant is able to bind to DNA-PKcs with indistinguishable affinity as WT ARTEMIS (Fig. 2*F*).

The ARM14 Mutant of ARTEMIS Does Not Possess Hairpin Opening, Endonuclease, or 5′-Exonuclease Activity—We tested the activity of ARM14 fractions collected from the Superose 12 column for nuclease action on a DNA hairpin and ssDNA substrates, specifically, a single-stranded poly(dT) substrate. The WT ARTEMIS endonuclease activity elutes as a symmetrical and defined peak. Unlike WT ARTEMIS protein, an equal amount of ARM14 mutant protein had no endonuclease activity on ssDNA (Fig. 2*E*, *lanes 2–5*). Importantly, no 5′-exonuclease activity was detected, as demonstrated by the lack of a band at the 1-nt position at the bottom of the gel (Fig. 3*A*, *lane 2 versus lane 3*). Therefore, the ARM14 mutant

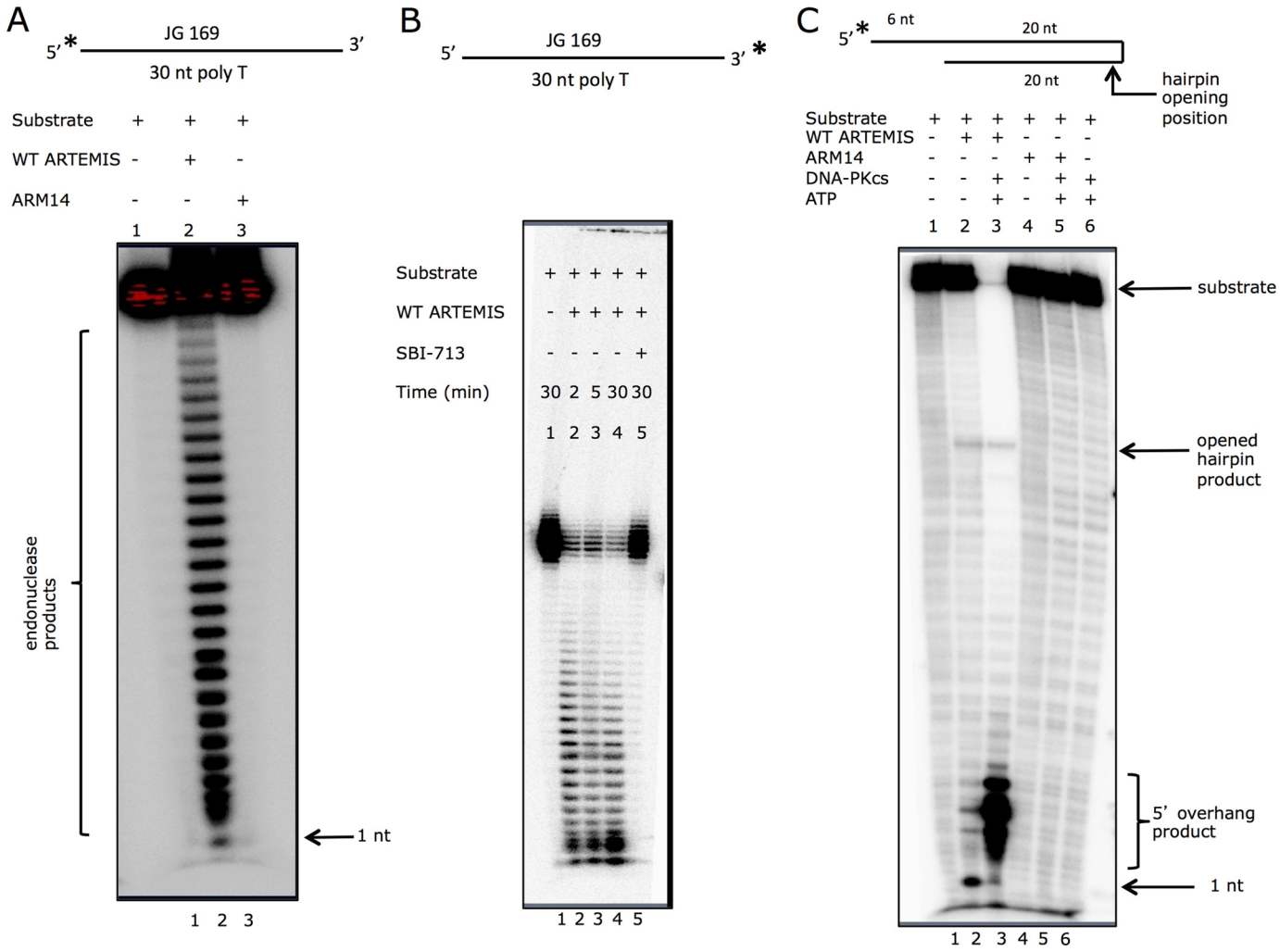

FIGURE 3. **Endonuclease and 5′-exonuclease activity of WT ARTEMIS and the ARTEMIS point mutant, ARM14.** *A*, the activity of ARM14 mutant was assayed for activity and compared with that of WT ARTEMIS. 50 nM ARM14 mutant or WT ARTEMIS was incubated with 50 nM ssDNA poly(dT) substrate in a 10-μl reaction. Reactions were incubated for 60 min at 37 °C, stopped, and run on 12% denaturing PAGE. The 5′-exonuclease activity is seen as the 1-nt product at the *bottom* of the gel. *B*, the activity of WT ARTEMIS was assayed for activity on a 3′-labeled substrate to determine the processitivity of the 5′-exonuclease activity. 50 nM WT ARTEMIS was incubated with 50 nM of ssDNA poly(dT) substrate (3′-labeled by terminal deoxynucleotidyl transferase) in a 10-μl reaction. Reactions were incubated for either 2, 5, or 30 min as indicated. Where compound SBI-713 is used, 20 μM was added to the reaction. *C*, 50 nM hairpin DNA substrate (YM164) was incubated with 50 nM WT ARTEMIS or 50 nM ARM14 in a 10-μl reaction. Reactions were incubated at 37 °C for 60 min. In lanes where DNA-PKcs was added, 50 nM DNA-PKcs, 0.5 mM of ATP, and 0.25 μM cold DNA YM8/9 were also added. *Lane 1* contains only the hairpin substrate. *Lane 2* contains ARTEMIS, which does have low dsDNA endonucleolytic activity without DNA-PKcs being present, but it has high 5′-exonucleolytic activity (1 nt product at *bottom* of gel). *Lanes 4* and *5* are the ARM14 point mutant of ARTEMIS. *Lane 3*, WT ARTEMIS plus DNA-PKcs, which generates a hairpin opened product, and 5′-overhang cleavage products. *Lane 6* is the control lane containing DNA-PKcs but no ARTEMIS.

does not exhibit any endonuclease activity or 5′-exonuclease activity.

In some DNA DSBs, the 5′ termini that are generated can be 5′-hydroxyl rather than 5′-phosphate. We tested for the ability of the intrinsic 5′-exonuclease activity of ARTEMIS to process a 3′-labeled substrate with a 5′-hydroxyl group. We labeled the substrate at the 3′ end by using terminal deoxynucleotidyl transferase and dATP that has a radioactive phosphate at the α position. To minimize addition of more than one radiolabeled mononucleotide, we include a 5-fold excess of ddTTP, which caps the 3′ terminus. However, the final substrate is a mixture of lengths due to incorporation of 1, 2, or 3 (and smaller amounts of more) radiolabels, followed by one dideoxy mononucleotide. We tested the processitivity of the 5′-exonuclease activity of ARTEMIS using this 3′-labeled substrate at three time points. Unlike processive nucleases, ARTEMIS is able to generate intermediate products even at the 30-min time point (Fig. 3*B*, *lane 4*). Therefore, ARTEMIS acts nonprocessively and can process 5′-hydroxyl termini as shown here (Fig. 3*B*) and substrates with 5′-phosphate termini, as we have shown previously (see Fig. 3*B* in Ref. 12).

We compared the activity of ARM14 with WT ARTEMIS on a hairpin substrate. To do this, we designed an oligonucleotide DNA substrate that is able to fold back on to itself upon annealing to form a hairpin substrate (YM164). WT ARTEMIS protein shows weak hairpin opening, weak endonuclease activity, as well as weak 5′-exonuclease activity on this substrate in Mg^{2+}-containing reactions that lack DNA-PKcs (Fig. 3*C*, *lane 2*). In contrast, the ARM14 protein generated no hairpin nicking, endonuclease products or 5′-exonuclease products even when we added DNA-PKcs to the reaction (Fig. 3*C*, *lane 5*).

The Endonuclease and 5′-Exonuclease Activities of ARTEMIS Can Be Inhibited in Parallel—We further tested the ability of selected compounds to inhibit the hairpin opening, endonuclease, and 5′-exonuclease activities of ARTEMIS. Prior to the high throughput screen, a small screen showed that ampicillin, a β-lactamase antibiotic that inhibits transpeptidase, is also inhibitory, probably because ARTEMIS is a member of the β-lactamase family. SBI-713 and SBI-116 are two structurally distinct <500 Da small molecules (data not shown) that were identified using a high throughput screen of a 31,000 compound subset of the National Institutes of Health Molecular Libraries Small Molecule Repository collection (Pubchem BioAssay AID 686956).

In the absence of any inhibitor, ARTEMIS has endonuclease activity as well as 5′-exonuclease activity on a hairpin substrate, YM164 (Fig. 4*A*, *lane 2*). However, at 20 μM, the SBI-713 dramatically inhibited both the endonuclease and the 5′-exonuclease activities of ARTEMIS (Fig. 4*A*, *lane 4*). However, 20 μM SBI-116 did not inhibit either activity (Fig. 4*A*, *lane 3*).

Given that ARTEMIS is an endonuclease, we wondered whether ARTEMIS cutting at the 5′ most nt could merely reflect a preferential cutting by ARTEMIS endonuclease activity. To distinguish this from its 5′-exonuclease activity, we utilized an ssDNA poly(dA) substrate. Single-stranded polypurine substrates are not endonucleolytically cut as efficiently by ARTEMIS, which prefers polypyrimidine single-stranded DNA substrates (9). From our previous work, we knew that the 5′-exonuclease activity of ARTEMIS is DNA-PKcs-independent (3). We tested the exonuclease activity of ARTEMIS in the presence and absence of DNA-PKcs (Fig. 4*B*, *lane 2 versus lane 3*). Consistent with our previous findings, we saw no difference in the exonuclease activity of purified WT ARTEMIS with or without DNA-PKcs. The addition of 20 μM of the inhibitor SBI-713 was able to inhibit the 5′-exonuclease activity of ARTEMIS, as demonstrated by the lack of the 1-nt exonuclease product (Fig. 4*B*, *lane 4*). This further demonstrates the 5′-exonuclease activity of ARTEMIS. Furthermore, we tested the ability of the ARM14 point mutant to process the poly(dA) ssDNA. The ARM14 mutant does not have any apparent endonuclease or 5′-exonuclease activity on this substrate when compared with WT ARTEMIS (Fig. 4*C*, *lane 3 versus lane 2*), indicating that the point mutation markedly reduces both endonuclease and 5′-exonuclease activities.

We also tested the inhibitors in titrations to determine whether the 5′-exonuclease and the endonuclease of ARTEMIS are inhibited over the same concentration ranges (Fig. 5). We found that as the concentration of ampicillin or SBI-713 increases, there is a concomitant inhibition of both the endonuclease and the 5′-exonuclease activity of ARTEMIS. The level of inhibition of the 5′ exo- and endonuclease activities is similar for both inhibitors. If the 5′-exonuclease were a contaminant, we would not expect both the ARTEMIS endonuclease and the contaminating 5′-exonuclease to be inhibited over the very same concentration ranges for each drug (Fig. 5).

We have also tested SBI-713 and ampicillin against other nucleases to assess specificity for inhibition of ARTEMIS. These included DNase I and micrococcal nuclease. SBI-713 does not inhibit either of these counterscreen nucleases (Fig. 4*D*).

In related studies, in 10 mM $MgCl_2$ reaction buffers, addition of $ZnCl_2$ above 10 μM inhibits ARTEMIS endonuclease activity (Fig. 6). It has been shown previously in certain cases that excess zinc can inhibit the enzymatic activity of zinc-dependent enzymes. This is thought to be caused by excess zinc-monohydroxide binding to the active form of the zinc-dependent enzyme, thereby preventing the catalytic site from binding active zinc (17). In the case of ARTEMIS, the inhibition by excess zinc is observed for the endonuclease activity as well as the 5′-exonuclease activity over the same Zn^{2+} concentration range (10 to 100 μM) (Fig. 6). This is consistent with the 5′-exonuclease activity of ARTEMIS sharing the same catalytic site as the endonuclease activity of ARTEMIS.

DISCUSSION

Although a 5′-DNA exonuclease activity co-purifies with ARTEMIS (Fig. 1), the 5′-exonuclease is not dependent on DNA-PKcs, whereas the ARTEMIS DNA endonuclease activities (5′- and 3′-overhang cleavage and hairpin opening) do depend on DNA-PKcs. For this reason, we did further studies described here to evaluate whether the 5′-exonuclease is intrinsic to ARTEMIS.

Here, we have provided several independent lines of evidence that the 5′-exonuclease is intrinsic to ARTEMIS. First, the 5′-exonuclease and the endonuclease activities co-fractionate.

Second, a point mutant of ARTEMIS is markedly reduced in 5′-exonuclease activity in the presence and absence of DNA-PKcs. A point mutant of ARTEMIS is very unlikely to affect any contaminating 5′-exonuclease. This alone is strong evidence of an intrinsic 5′-exonuclease.

Third, both the endonuclease and the 5′-exonuclease activity of ARTEMIS can be inhibited by small molecules that are not chelators. It is unlikely that any one inhibitor is able to inhibit both ARTEMIS endonuclease activity and an unidentified contaminating 5′-exonuclease. It is even more unlikely that these specific inhibitors would affect a contaminating 5′-exonuclease at the same concentrations as they affect ARTEMIS endonuclease activity.

Fourth, disruption of the catalytic sites by divalent cation replacement is known to alter the activity of enzymes in the metallo-β-lactamase family of nucleases (18). We found that the addition of excess zinc (>10 μM) to the reaction buffer decreases the endonuclease as well as the 5′-exonuclease activity of ARTEMIS. It seems unlikely that a contaminating 5′-exonuclease would also show this behavior, particularly at the same low (micromolar) concentrations of Zn^{2+}.

Fifth, we explored the possibility that the 5′-exonuclease activity seen in our gels is actually the result of the ARTEMIS endonuclease activity acting on the 5′-terminal nucleotide. We created a poly(dA) ssDNA substrate that is not as readily endonucleolytically processed by the ARTEMIS endonuclease activity but conceivably might be processed by the 5′-exonuclease activity of ARTEMIS. Indeed, we do observe 5′-exonuclease activity when using this poly(dA) ssDNA substrate, indicating that the activity seen at the 5′ end on a polypyrimidine substrate is attributable to 5′-exonuclease activity and not merely due to

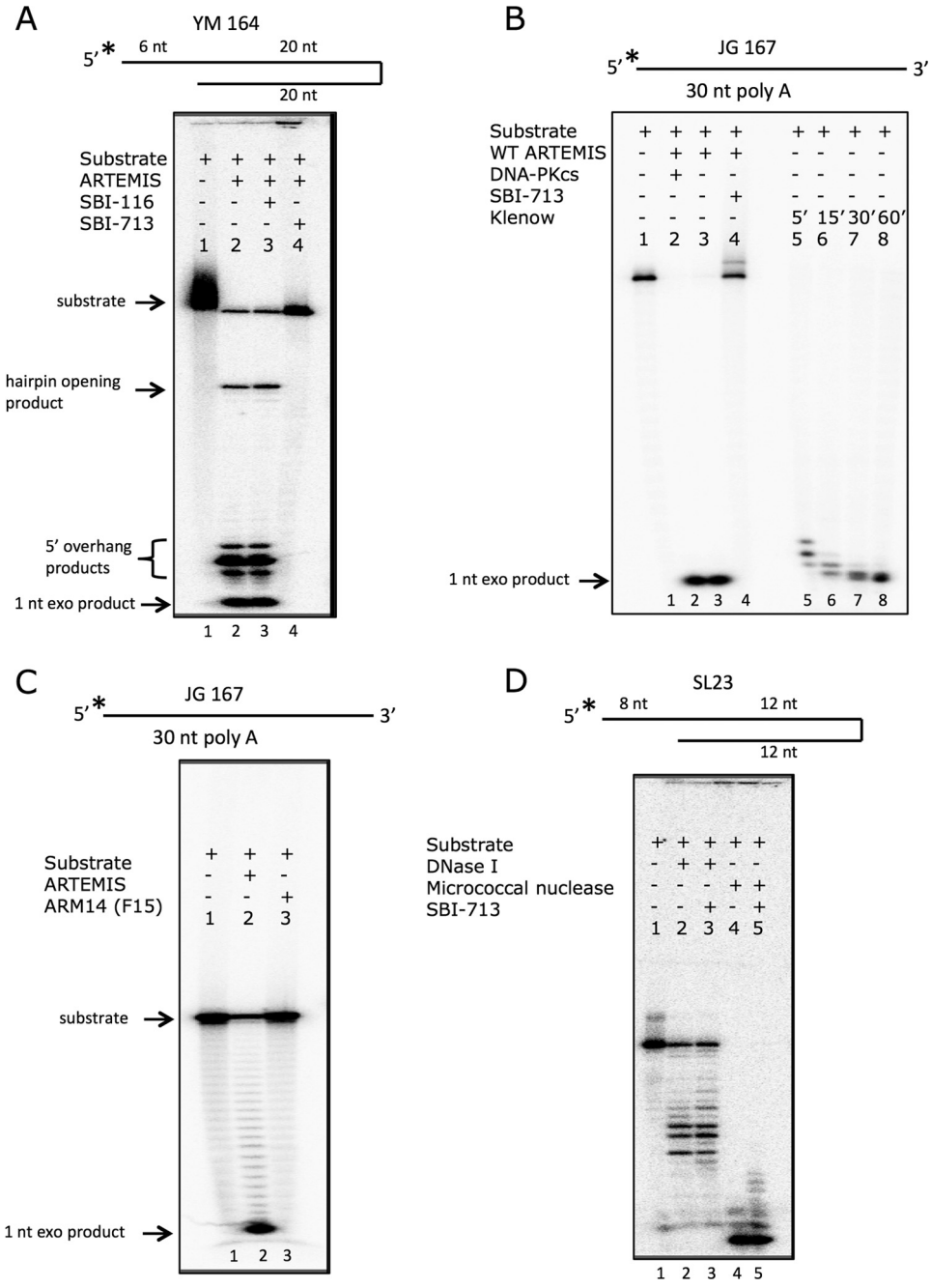

FIGURE 4. **Small molecule inhibitors block both the 5′-exonuclease and the endonucleolytic activities of ARTEMIS on hairpin DNA.** *A*, addition of compound SBI-713 inhibits the endonuclease and 5′-exonuclease activities of ARTEMIS. 50 nM hairpin DNA substrate (YM164) was incubated with 60 nM ARTEMIS in a 10-μl reaction with the buffer as described under "Experimental Procedures," except that 10 mM $MnCl_2$ is replaced for $MgCl_2$ in *A* only. Reactions were incubated at 37 °C for 60 min. Compound SBI-116 or SBI-713 was added at 20 μM in the indicated reactions. The 5′-exonuclease activity is seen as the 1-nt product at the *bottom* of the gel. *B*, ARTEMIS has weak endonuclease activity on a single-stranded poly(dA) substrate but has 5′-exonuclease activity. 50 nM ssDNA substrate (JG167) was incubated with 60 nM ARTEMIS in addition to 75 nM DNA-PKcs and 0.5 mM ATP where applicable. 20 μM inhibitor SBI-713 was added to the indicated reactions. Reactions were incubated for 1 h at 37 °C. The 5′-exonuclease activity is seen as the 1-nt product at the *bottom* of the gel. The Klenow ladder was generated by adding 2 units of Klenow (New England Biolabs) to 50 nM substrate JG 167. Reactions were incubated for the indicated time periods at 37 °C. *C*, point mutant ARM14 does not have endonuclease or 5′-exonuclease activity on poly(dA) substrate. 50 nM ssDNA substrate (JG167) was incubated with 60 nM ARTEMIS or 60 nM ARM14 point mutant. Reactions were incubated for 1 h at 37 °C. The 5′-exonuclease (*exo*) activity is seen as the 1-nt product at the *bottom* of the gel. *D*, the specificity of compound SBI-713 was tested against DNase I and micrococcal nuclease. 100 nM DNase I or 2.5 μM micrococcal nuclease (Sigma) was incubated with 20 nM of the hairpin substrate SL23. Where indicated, 20 μM of SBI-713 was added to the reaction. Reactions were incubated for 1 h at 37 °C in the manufacturer's buffer.

the endonuclease activity of ARTEMIS. Importantly, this 5′-exonuclease activity is completely inhibited by the SBI-713 compound (Fig. 4). From the evidence presented here, we conclude that the 5′-exonuclease activity seen in purified ARTEMIS is intrinsic to the ARTEMIS protein and not due to a co-purifying contaminating enzyme.

The metallo-β-lactamase family of nucleases uses several conserved catalytic residues to coordinate divalent cations. The

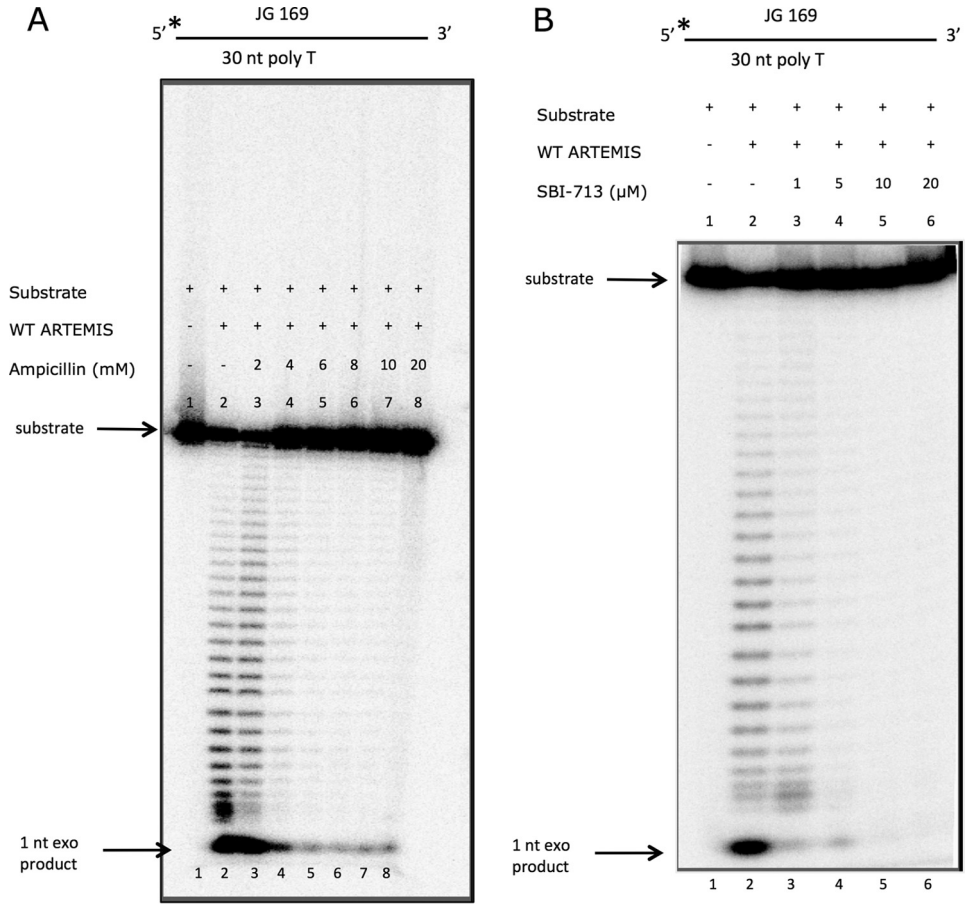

FIGURE 5. **Titration of inhibition of ARTEMIS endonuclease and 5′-exonuclease activities by small molecule inhibitors.** *A*, addition of ampicillin inhibits the large majority of the endonuclease and 5′-exonuclease (*exo*) activities of ARTEMIS in parallel. The ssDNA substrate (50 nM JG169) was incubated with 50 nM ARTEMIS in a 10-μl reaction. Ampicillin was added in concentration(s) as indicated. Reactions were incubated at 37 °C for 30 min, stopped, and analyzed by 12% denaturing PAGE. Quantitation indicates that similarly low levels of both the endonuclease and the 5′-exonuclease activity (1-nt product) escape inhibition by ampicillin. *B*, addition of the compound SBI-713 inhibits Artemis on a single-stranded poly(dT) substrate. The ssDNA substrate (50 nM JG169) was incubated with 50 nM ARTEMIS in a 10-μl reaction. SBI-713 was added in concentration(s) as indicated. Reactions were incubated at 37 °C for 30 min, stopped, and analyzed by 12% denaturing PAGE. SBI-713 inhibition of both the 5′-exonuclease and the endonuclease is complete at 10 and 20 μM. A small level of residual 5′-exonuclease and endonuclease persists even at the highest levels of ampicillin tested.

two most conserved residues within the catalytic site are histidine and aspartic acid (14). We generated the ARM14 point mutant, which changed a conserved histidine residue to an alanine residue. If both the endonuclease activity of ARTEMIS and 5′-exonuclease activity of ARTEMIS shared a common catalytic site, by disrupting the divalent ligand in the site there should be a corresponding decrease in both endonuclease as well as the 5′-exonuclease activity of ARTEMIS, and this is what we observe here.

We have previously purified ARM14 mutant from 293T cells using a two-step purification. Although this point mutant is inactive for the hairpin opening and endonuclease activity on a hairpin substrate, this version of ARM14 appeared to still retain most of the 5′-exonuclease activity (13). We attribute the discrepancies in our findings with insect cell-purified ARM14 in the current study to our earlier study to the high levels of contaminating nucleases in mammalian cells that are difficult to remove during purification. The baculovirus system for ARTEMIS production here contains much lower levels of background contaminating nucleases, which can be subsequently removed in our three step purification.

Using a purification process consisting of phosphocellulose, Ni-NTA-agarose, and hydroxyapatite, one group separated the usual bulk of other cellular 5′-exonuclease activity away from the endonuclease activity of ARTEMIS (19). They concluded that the 5′-exonuclease activity was not intrinsic to ARTEMIS based on an assay that was much less sensitive than our assay. Even at their reduced sensitivity, we note that some 5′-exonuclease activity is still apparent in their assay gels, which they did not point out (19). For example, they tested their purified ARTEMIS on a single-stranded 5′ radiolabeled DNA substrate to assay for 5′-exonuclease activity (Fig. 5*B* of Ref. 19). Although they could detect no 5′-exonuclease activity, their assay was insensitive to the extent that they also could not detect any of the single-stranded endonuclease activity of ARTEMIS (19). This was due in part to exposure intensities of their gels that were 10- to 20-fold lower than what we use to detect both single-stranded endo- and 5′-exonuclease activities (12). Despite the fact that their gels show apparent residual 5′-exonuclease activity at their darker radiolabel exposures (Fig. 5*C*, lanes 10 & 11 in ref. (19)), they nevertheless concluded that ARTEMIS has no intrinsic 5′-exonuclease activity (19).

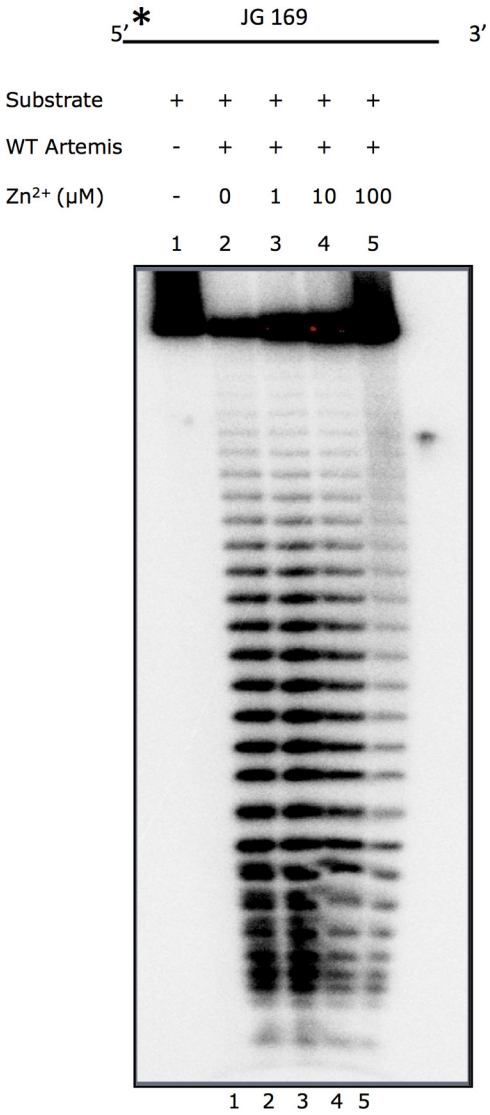

FIGURE 6. **Inhibition of ARTEMIS endonuclease and 5′-exonuclease activity by Zn^{2+}.** Addition of Zn^{2+} inhibits the endonuclease and 5′-exonuclease activity of ARTEMIS in parallel. 50 nM ssDNA substrate (JG169) was incubated with 50 nM ARTEMIS in a 10-μl reaction. Reactions were incubated at 37 °C for 60 min. Reactions were stopped and analyzed by 12% denaturing PAGE.

Other members of the metallo-β-lactamase family possess nuclease activities similar to those of ARTEMIS. CPSF-73, an enzyme involved in the 3′ end processing of histone pre-mRNA, has been shown to possess endonuclease activity as well as 5′-exonuclease activity on single-stranded RNA substrates (18, 20). The nuclease activities of CPSF-73 can be abolished by the addition of zinc specific chelators. We find that ARTEMIS nuclease activities (both endo- and 5′-exonuclease) are abolished by addition of these same zinc-specific chelators (data not shown), suggesting that members of this family use the same divalent cations in the catalytic site (21). Biochemical studies have also demonstrated that human SMN1A and SMN1B proteins, also members of the metallo-β-lactamase family and involved in inter-strand cross-link DNA repair, are capable of acting as a 5′-exonuclease on single-stranded and double-stranded DNA substrates (16), and this is its only biochemically defined enzymatic activity. Mutations of key catalytic residues within the metallo-β-lactamase domain also abolish the 5′-3′-DNA processing ability of hSMN1a and hSMN1b. Therefore, 5′-exonuclease activity is intrinsic to many members of the metallo-β-lactamase nuclease family, and the catalytic site involved during DNA processing resides in the metallo-β-lactamase domain. Our current study clearly shows that ARTEMIS also has a similar 5′-exonuclease activity.

The 5′-exonuclease activity described here would permit ARTEMIS to act on 1- and 2-nt 5′-overhangs more efficiently because such short 5′-overhangs are not optimal substrates for action by ARTEMIS in an endonucleolytic manner (3). This would be of particular utility for repair of ionizing radiation damage, which might have short overhangs with either a 5′-phosphate or 5′-hydroxyl.

Acknowledgments—We thank Dr. Ray Mosteller (University of Southern California) and members of the Lieber lab for critically reading the manuscript. We thank Dr. Ralf Langen (University of Southern California) for help obtaining the CD spectra. We thank Dr. David Auld (Harvard University) and Dr. Andrew Mason (California State University, Long Beach) for advice about zinc metalloenzymes. We thank Fusayo Yamamoto and Drs. T. C. Chung (Sanford-Burnham Research Institute) for conducting the high throughput screen of ARTEMIS inhibitors.

REFERENCES

1. Dronkert, M. L., de Wit, J., Boeve, M., Vasconcelos, M. L., van Steeg, H., Tan, T. L., Hoeijmakers, J. H., and Kanaar, R. (2000) Disruption of mouse SNM1 causes increased sensitivity to the DNA interstrand cross-linking agent mitomycin C. *Mol. Cell. Biol.* **20,** 4553–4561
2. van Overbeek, M., and de Lange, T. (2006) Apollo, an Artemis-related nuclease, interacts with TRF2 and protects human telomeres in S phase. *Curr. Biol.* **16,** 1295–1302
3. Ma, Y., Pannicke, U., Schwarz, K., and Lieber, M. R. (2002) Hairpin opening and overhang processing by an Artemis:DNA-PKcs complex in V(D)J recombination and in nonhomologous end joining. *Cell* **108,** 781–794
4. Moshous, D., Callebaut, I., de Chasseval, R., Corneo, B., Cavazzana-Calvo, M., Le Diest, F., Tezcan, I., Sanal, O., Bertrand, Y., Philippe, N., Fischer, A., and de Villartay, J. P. (2001) Artemis, a novel DNA double-strand break repair/V(D)J recombination protein, is mutated in human severe combined immune deficiency. *Cell* **105,** 177–186
5. Lieber, M. R. (2010) The mechanism of double-strand DNA break repair by the nonhomologous DNA end-joining pathway. *Annu. Rev. Biochem.* **79,** 181–211
6. Riballo, E., Kühne, M., Rief, N., Doherty, A., Smith, G. C., Recio, M. J., Reis, C., Dahm, K., Fricke, A., Krempler, A., Parker, A. R., Jackson, S. P., Gennery, A., Jeggo, P. A., and Löbrich, M. (2004) A pathway of double-strand break rejoining dependent upon ATM, Artemis, and proteins locating to gamma-H2AX foci. *Mol. Cell* **16,** 715–724
7. Rooney, S., Alt, F. W., Lombard, D., Whitlow, S., Eckersdorff, M., Fleming, J., Fugmann, S., Ferguson, D. O., Schatz, D. G., and Sekiguchi, J. (2003) Defective DNA repair and increased genomic instability in Artemis-deficient murine cells. *J. Exp. Med.* **197,** 553–565
8. Kurosawa, A., Koyama, H., Takayama, S., Miki, K., Ayusawa, D., Fujii, M., Iiizumi, S., and Adachi, N. (2008) The requirement of Artemis in double-strand break repair depends on the type of DNA damage. *DNA Cell Biol.* **27,** 55–61
9. Lu, H., Shimazaki, N., Raval, P., Gu, J., Watanabe, G., Schwarz, K., Swanson, P. C., and Lieber, M. R. (2008) A biochemically defined system for coding joint formation in human V(D)J recombination. *Mol. Cell* **31,** 485–497
10. Yannone, S. M., Khan, I. S., Zhou, R. Z., Zhou, T., Valerie, K., and Povirk, L. F. (2008) Coordinate 5′ and 3′ endonucleolytic trimming of terminally

blocked blunt DNA double-strand break ends by Artemis nuclease and DNA-dependent protein kinase. *Nucleic Acids Res.* **36,** 3354–3365
11. Niewolik, D., Pannicke, U., Lu, H., Ma, Y., Wang, L. C., Kulesza, P., Zandi, E., Lieber, M. R., and Schwarz, K. (2006) DNA-PKcs dependence of ARTEMIS endonucleolytic activity: differences between hairpins and 5′ or 3′ overhangs. *J. Biol. Chem.* **281,** 33900–33909
12. Gu, J., Li, S., Zhang, X., Wang, L. C., Niewolik, D., Schwarz, K., Legerski, R. J., Zandi, E., and Lieber, M. R. (2010) DNA-PKcs regulates a single-stranded DNA endonuclease activity of Artemis. *DNA Repair* **9,** 429–437
13. Pannicke, U., Ma, Y., Hopfner, K. P., Niewolik, D., Lieber, M. R., and Schwarz, K. (2004) Functional and biochemical dissection of the structure-specific nuclease ARTEMIS. *EMBO J.* **23,** 1987–1997
14. Aravind, L. (1999) An evolutionary classification of the metallo-β-lactamase fold proteins. *In Silico Biol.* **1,** 69–91
15. Chan, D. W., Mody, C. H., Ting, N. S., and Lees-Miller, S. P. (1996) Purification and characterization of the double-stranded DNA-activated protein kinase, DNA-PK, from human placenta. *Biochem. Cell Biol.* **74,** 67–73
16. Sengerová, B., Allerston, C. K., Abu, M., Lee, S. Y., Hartley, J., Kiakos, K., Schofield, C. J., Hartley, J. A., Gileadi, O., and McHugh, P. J. (2012) Characterization of the human SNM1A and SNM1B/Apollo DNA repair exonucleases. *J. Biol. Chem.* **287,** 26254–26267
17. Larsen, K. S., and Auld, D. S. (1989) Carboxypeptidase A: mechanism of zinc inhibition. *Biochemistry* **28,** 9620–9625
18. Dominski, Z. (2007) Nucleases of the metallo-beta-lactamase family and their role in DNA and RNA metabolism. *Crit. Rev. Biochem. Mol. Biol.* **42,** 67–93
19. Pawelczak, K. S., and Turchi, J. J. (2010) Purification and characterization of exonuclease-free Artemis: Implications for DNA-PK-dependent processing of DNA termini in NHEJ-catalyzed DSB repair. *DNA Repair* **9,** 670–677
20. Mandel, C. R., Kaneko, S., Zhang, H., Gebauer, D., Vethantham, V., Manley, J. L., and Tong, L. (2006) Polyadenylation factor CPSF-73 is the pre-mRNA 3′-end-processing endonuclease. *Nature* **444,** 953–956
21. Ryan, K., Calvo, O., and Manley, J. L. (2004) Evidence that polyadenylation factor CPSF-73 is the mRNA 3′ processing endonuclease. *Rna* **10,** 565–573